



Cite this: *Metallomics*, 2018, 10, 287

The P-type ATPase inhibiting potential of polyoxotungstates†

Nadiia Gumerova,^a Lukáš Krivosudský,^{‡a} Gil Fraqueza,^{bc} Joscha Breibeck,^a Emir Al-Sayed,^a Elias Tanuhadi,^a Aleksandar Bijelic,^a Juan Fuentes,^b Manuel Aureliano^{*bd} and Annette Rompel^{*a}

Polyoxometalates (POMs) are transition metal complexes that exhibit a broad diversity of structures and properties rendering them promising for biological purposes. POMs are able to inhibit a series of biologically important enzymes, including phosphatases, and thus are able to affect many biochemical processes. In the present study, we analyzed and compared the inhibitory effects of nine different polyoxotungstates (POTs) on two P-type ATPases, Ca^{2+} -ATPase from skeletal muscle and Na^+/K^+ -ATPase from basal membrane of skin epithelia. For Ca^{2+} -ATPase inhibition, an *in vitro* study was performed and the strongest inhibitors were determined to be the large heteropolytungstate $\text{K}_9(\text{C}_2\text{H}_8\text{N})_5[\text{H}_{10}\text{Se}_2\text{W}_{29}\text{O}_{103}]$ (Se_2W_{29}) and the Dawson-type POT $\text{K}_6[\alpha\text{-P}_2\text{W}_{18}\text{O}_{62}]$ (P_2W_{18}) exhibiting IC_{50} values of 0.3 and 0.6 μM , respectively. Promising results were also shown for the Keggin-based POTs $\text{K}_6\text{H}_2[\text{CoW}_{11}\text{TiO}_{40}]$ (CoW_{11}Ti , $\text{IC}_{50} = 4 \mu\text{M}$) and $\text{Na}_{10}[\alpha\text{-SiW}_9\text{O}_{34}]$ (SiW_9 , $\text{IC}_{50} = 16 \mu\text{M}$), $\text{K}_{14}[\text{As}_2\text{W}_{19}\text{O}_{67}(\text{H}_2\text{O})]$ (As_2W_{19} , $\text{IC}_{50} = 28 \mu\text{M}$) and the lacunary Dawson $\text{K}_{12}[\alpha\text{-H}_2\text{P}_2\text{W}_{12}\text{O}_{48}]$ (P_2W_{12} , $\text{IC}_{50} = 11 \mu\text{M}$), whereas low inhibitory potencies were observed for the isopolytungstate $\text{Na}_{12}[\text{H}_4\text{W}_{22}\text{O}_{74}]$ (W_{22} , $\text{IC}_{50} = 68 \mu\text{M}$) and the Anderson-type $\text{Na}_6[\text{TeW}_6\text{O}_{24}]$ (TeW_6 , $\text{IC}_{50} = 200 \mu\text{M}$). Regarding the inhibition of Na^+/K^+ -ATPase activity, for the first time an *ex vivo* study was conducted using the opercular epithelium of killifish in order to investigate the effects of POTs on the epithelial chloride secretion. Interestingly, 1 μM of the most potent Ca^{2+} -ATPase inhibitor, Se_2W_{29} , showed only a minor inhibitory effect (14% inhibition) on Na^+/K^+ -ATPase activity, whereas almost total inhibition (99% inhibition) was achieved using P_2W_{18} . The remaining POTs exhibited similar inhibition rates on both ATPases. These results reveal the high potential of some POTs to act as P-type ATPase inhibitors, with Se_2W_{29} showing high selectivity towards Ca^{2+} -ATPase.

Received 30th September 2017,
Accepted 30th November 2017

DOI: 10.1039/c7mt00279c

rsc.li/metallomics

Significance to metallomics

We studied the inhibitory effects of nine different polyoxotungstates (POTs) on P-type ATPases *in vitro* (Ca^{2+} -ATPase) and *ex vivo* (Na^+/K^+ -ATPase). The study reveals that some POTs like the Dawson anion $[\text{P}_2\text{W}_{18}\text{O}_{62}]^{6-}$, which was highly active *in vitro* and *ex vivo*, are potent ATPase inhibitors. Furthermore, there is a charge density-activity correlation for the most potent POTs ($\text{IC}_{50} < 16 \mu\text{M}$), namely Se_2W_{29} , P_2W_{18} , CoW_{11}Ti , SiW_9 and P_2W_{12} . As P-type ATPases represent pharmacologically important targets due to their important role in health and disease, the here reported bioactive POTs should be considered as possible future metallodrugs.

Introduction

Polyoxometalates (POMs) are metal clusters¹ that exhibit a broad diversity of structures and outstanding properties leading to their application in various fields such as catalysis,^{2,3} photochemistry,⁴ material science,^{5,6} macromolecular crystallography^{7–15} and medicine.^{16–22} POMs can be divided into isopolyanions (IPAs), which consist only of one type of metal atom ($\text{M} = \text{addenda atom}$), $[\text{M}_m\text{O}_y]^{q-}$, and heteropolyanions (HPAs), which contain one or more additional elements ($\text{X} = \text{heteroatom}$), $[\text{X}_m\text{M}_m\text{O}_y]^{q-}$. The most common representative of IPAs is the Lindqvist structure,

^a Universität Wien, Fakultät für Chemie, Institut für Biophysikalische Chemie, Althanstraße 14, 1090 Wien, Austria. E-mail: annette.rompel@univie.ac.at; Web: www.bpc.univie.ac.at

^b Centre of Marine Sciences, University of Algarve, 8005-139 Faro, Portugal

^c Institute of Engineering, University of Algarve, 8005-139 Faro, Portugal

^d Faculty of Sciences and Technology, University of Algarve, 8005-139 Faro, Portugal. E-mail: maalves@ualg.pt

† Electronic supplementary information (ESI) available: Positive control experiment for Na^+/K^+ -ATPase inhibition of ouabain. See DOI: 10.1039/c7mt00279c

‡ On leave from: Comenius University, Faculty of Natural Sciences, Department of Inorganic Chemistry, Mlynská dolina, Ilkovičova 6, 842 15 Bratislava, Slovakia.



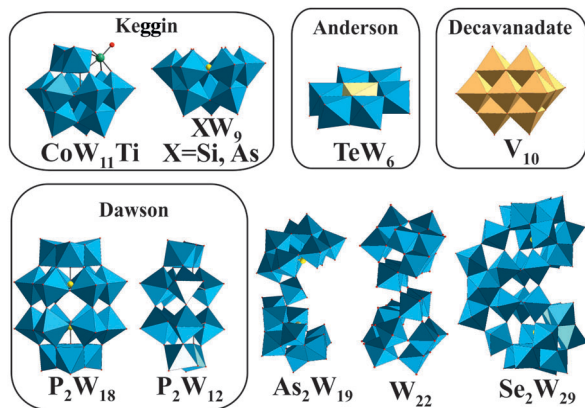


Fig. 1 Structures of the investigated POTs (Table 1) and $[V_{10}O_{28}]^{6-}$. Color code: WO_6 , blue polyhedra; VO_6 , dark yellow polyhedra; heteroatom, light yellow sphere or polyhedra; Ti as substituted atom, green sphere.

whereas the well-known Dawson, Keggin and Anderson archetypes belong to the HPAs (Fig. 1). POM research represents an emerging field and especially bioactive POMs are getting more and more attractive due to their ability to interact with important enzymes like alkaline phosphatases, ecto-nucleotidases and ATPases and their potential to interfere with specific cellular processes, such as mitochondria respiration.^{21–24} POMs like decavanadate or Keggin-type polyoxotungstates (POTs) and polyoxomolybdates are currently the focus of biological and biomedical research as they show promising antibacterial and antidiabetic activities,^{21,22,24–28} whereas only few biological studies exist for other POM archetypes such as the Anderson structure.²⁹

The main role of the sarcoplasmic reticulum (SR) Ca^{2+} -ATPase is translocation of cellular Ca^{2+} from the cytoplasm to the SR, which is involved in muscle relaxation.^{30,31} However, Ca^{2+} -ATPase is globally associated with cellular calcium homeostasis, a process of ion transport that is coupled with ATP hydrolysis. ATP hydrolysis follows a well-known mechanism traversing at least four intermediate steps and two protein conformations, namely E1 and E2, with E1 being the conformation with high affinity for the exported substrate and E2 the form with high affinity for the imported substrate.^{30,31} As SR vesicles from skeletal muscle contain a large amount of Ca^{2+} -ATPase, they represent a useful *in vitro* model to study the effects of drugs and POMs on calcium homeostasis.^{32,33} To our knowledge, only a few POMs, such as decavanadate (V_{10}) and decaniobate (Nb_{10}), were described to be

potent non-competitive inhibitors ($IC_{50} = 15$ and $35 \mu M$, respectively) of the hydrolytic activity of SR Ca^{2+} -ATPase.³³ Na^+/K^+ -ATPase transports Na^+ out of the cell while pumping K^+ into cells and is thus responsible for the ionic and osmotic balance in cells and an important transducer of signals. As all P-type ATPases, the Na^+/K^+ pump derives energy from ATP hydrolysis.

Herein, we report and compare the effects of nine different POTs (Fig. 1 and Table 1) on the *in vitro* activity of Ca^{2+} -ATPase from SR. For the first time, we investigate the effects of POTs on the process of epithelial chloride secretion, energized by the activity of basolateral Na^+/K^+ -ATPase, using an *ex vivo* model obtained from basal membrane of epithelial skin (killifish). Putative correlations between the inhibitory activity of POTs (IC_{50} values), their charge density and size were derived. The results reveal that some POTs are potent inhibitors of P-type ATPases even under almost physiological conditions (*ex vivo* study) and therefore should be taken into consideration as P-type ATPase targeting drugs. One POT, namely $\text{K}_9(\text{C}_2\text{H}_8\text{N})_5[\text{H}_{10}\text{Se}_2\text{W}_{29}\text{O}_{103}]$ (Se_2W_{29}) showed clear selectivity towards one pump (Ca^{2+} -ATPase), whereas other POTs like the Anderson archetype $\text{Na}_6[\text{TeW}_6\text{O}_{24}]$ showed very low inhibition on both ion pumps.

Experimental section

Polyoxometalates

The POTs used in this study, $\text{K}_6[\alpha\text{-P}_2\text{W}_{18}\text{O}_{62}]\cdot 14\text{H}_2\text{O}$,³⁵ $\text{Na}_6\text{-}[\text{TeW}_6\text{O}_{24}]\cdot 22\text{H}_2\text{O}$,³⁶ $\text{K}_6\text{H}_2[\text{TiW}_{11}\text{CoO}_{40}]\cdot 13\text{H}_2\text{O}$,³⁷ $\text{Na}_{10}[\alpha\text{-SiW}_9\text{O}_{34}]\cdot 16\text{H}_2\text{O}$,³⁵ $\text{Na}_9[\alpha\text{-AsW}_9\text{O}_{33}]\cdot 27\text{H}_2\text{O}$,³⁸ $\text{K}_{12}[\alpha\text{-H}_2\text{P}_2\text{W}_{12}\text{O}_{48}]\cdot 16\text{H}_2\text{O}$,³⁵ $\text{K}_{14}[\text{As}_2\text{W}_{19}\text{O}_{67}(\text{H}_2\text{O})]\cdot 23\text{H}_2\text{O}$,³⁹ $\text{K}_9(\text{C}_2\text{H}_8\text{N})_5[\text{H}_{10}\text{Se}_2\text{W}_{29}\text{O}_{103}]\cdot 30\text{H}_2\text{O}$ ⁴⁰ and $\text{Na}_{12}[\text{H}_4\text{W}_{22}\text{O}_{74}]\cdot 50\text{H}_2\text{O}$ ⁴¹ (Table 1 and Fig. 1), were synthesized according to published procedures (see references in Table 1) and their identity was confirmed by infrared spectroscopy. Stock solutions of POTs were freshly prepared by dissolving the solid compound in water and keeping the solution on ice to avoid POT decomposition. The concentrations of the stock solutions were 10 mM and 1 mM for all POTs except for Se_2W_{29} (1 mM and 0.1 mM).

Preparation of sarcoplasmic reticulum Ca^{2+} -ATPase vesicles

All reagents used for the preparation of the calcium pump vesicles were purchased from Sigma-Aldrich (Portugal). Isolated sarcoplasmic reticulum vesicles (SRVs), prepared from rabbit skeletal muscles as described elsewhere,³³ were suspended in

Table 1 Structural/molecular features of the POTs used in this study

POTs (abbreviated)	Sum formula	M_r	Charge	POT archetype	Ref.
P ₂ W ₁₈	K ₆ [α -P ₂ W ₁₈ O ₆₂] \cdot 14H ₂ O	4849.83	6 $-$	Dawson	35
TeW ₆	Na ₆ [TeW ₆ O ₂₄] \cdot 22H ₂ O	2148.56	6 $-$	Anderson-Evans	36
CoW ₁₁ Ti	K ₆ H ₂ [TiW ₁₁ CoO ₄₀] \cdot 13H ₂ O	3239.62	8 $-$	Mono-substituted Keggin	37
AsW ₉	Na ₉ [B- α -AsW ₉ O ₃₃] \cdot 27H ₂ O	2950.37	9 $-$	Tri-lacunary Keggin	38
SiW ₉	Na ₁₀ [A- α -SiW ₉ O ₃₄] \cdot 16H ₂ O	2744.52	10 $-$	Tri-lacunary Keggin	35
P ₂ W ₁₂	K ₁₂ [α -H ₂ P ₂ W ₁₂ O ₄₈] \cdot 16H ₂ O	3795.19	12 $-$	Lacunary Dawson	35
As ₂ W ₁₉	K ₁₄ [As ₂ W ₁₉ O ₆₇ (H ₂ O)] \cdot 23H ₂ O	5694.15	14 $-$	Doubled anion based on tri-lacunary Keggin anions	39
Se ₂ W ₂₉	K ₉ (C ₂ H ₈ N) ₅ [H ₁₀ Se ₂ W ₂₉ O ₁₀₃] \cdot 30H ₂ O	8270.09	14 $-$	Lacunary anion based on two tri-lacunary Keggin anions containing {(WO ₇)W ₄ } pentagonal unit	40
W ₂₂	Na ₁₂ [H ₄ W ₂₂ O ₇₄] \cdot 50H ₂ O	6409.10	12 $-$	Dimeric isopolyanion based on two {W ₁₁ } units	41

0.1 M KCl, 10 mM HEPES (pH 7.0), diluted 1:1 with 2.0 M sucrose and frozen in liquid nitrogen for storage at -80°C . The protein concentration was determined spectrophotometrically at 595 nm in the presence of 0.125% of sodium dodecyl sulphate (SDS) by Bradford method with bovine serum albumin as a standard. The percentage of each protein present in the SRV preparations was determined by densitometry analysis of SDS-PAGE (7.5% acrylamide) protein bands. The SR Ca^{2+} -ATPase constituted at least 70% of the total protein amount in the SR-vesicles according to SDS-PAGE. The sarcoplasmic reticulum Ca^{2+} -ATPase-1 (SERCA-1) was the predominant isoform in our SR preparations.⁴²

Effects of POTs on ATP hydrolysis of SR Ca^{2+} -ATPase

Steady-state assays of the SR Ca^{2+} -ATPase were measured spectrophotometrically at 25°C using the coupled enzyme pyruvate kinase/lactate dehydrogenase assay (Scheme 1) as described elsewhere.⁴² Briefly, after the addition of the enzymes (pyruvate kinase and lactate dehydrogenase) and the substrate phosphoenolpyruvate to the medium, the experiment was initiated by adding NADH (0.25 mM) and the vesicles containing Ca^{2+} -ATPase ($10\text{ }\mu\text{g mL}^{-1}$).

ATP (2.5 mM) was added and the absorbance was recorded for about 1 minute (basal activity). Afterwards, the calcium ionophore calcimycin 4% (w/w), which releases again the Ca^{2+} ions, that were pumped in by the ATPase, was added and the decreasing NADH absorbance at 340 nm was measured for about 2 minutes (uncoupled ATPase activity). This was done to increase the ATPase activity (due to the ionophore-mediated impairment of the Ca^{2+} gradient) in order to better study the effect of the inhibitors and to ensure that the SR Ca^{2+} -ATPase vesicles are not leaky. For the experiments including POTs, freshly prepared POT solutions (10 mM and 1 mM for all POTs except for Se_2W_{29} , 1 mM and 0.1 mM) were added to the medium prior to the addition of SR Ca^{2+} -ATPase. The ATPase activity and its inhibition was measured taking into account the decrease of the OD (optical density) per minute in the absence (100%) and in the presence of the investigated POTs.³³ The detection system was not affected by the POTs themselves (not even at their highest concentrations), which was confirmed by a rapid decrease in absorbance at 340 nm upon addition of $40\text{ }\mu\text{M}$ ADP after the assay. All experiments were performed at least in triplicates. The inhibitory power of the investigated

POTs was evaluated by determining the respective IC_{50} value, that is, the POT concentration needed to induce a 50% inhibition of the Ca^{2+} -ATPase enzyme activity.

Animals used for *ex vivo* studies

Killifish (*F. heteroclitus*, 4–8 g) were collected with fish traps from the saltmarshes of Ria Formosa (Faro, Portugal) and maintained in Ramalhete Marine Station (CCMar, University of Algarve, Faro, Portugal) with running seawater (35 ppt) at a density of $<5\text{ kg m}^{-3}$, $18\text{--}20^{\circ}\text{C}$ and 12:12 h light:dark photoperiod. The animals were handfed twice daily (final ratio of 2% of the body weight) with commercially available dry pellets (Sorgal, Portugal). The fishes were then food deprived for 24 h before sampling. The animal collections (ICN, Portugal) and the experimental procedures comply with the guidelines of the European Union Council (86/609/EU) for the use of laboratory animals. All animal protocols were performed under a “Group C” license from the Direção-Geral de Veterinária, Ministério da Agricultura, do Desenvolvimento Rural e das Pescas, Portugal.

Epithelial short circuit current in Ussing chambers *ex vivo*

Epithelial tissues can transport ions and generate a transepithelial voltage termed “active transport potential”, which is caused by the asymmetric distribution of ion channels and transporters on the apical and basolateral membranes. The net movement of charges from the apical to the basolateral side (and *vice versa*) generates a voltage equal to the voltage differences between the apical and basolateral membranes. *Ex vivo*, the short circuit current (I_{sc}) is an accurate reflection of the secretory/absorptive capacity of the tissue when short-circuited. In the opercular epithelium of killifish used for our studies, I_{sc} is a direct measure of apical chloride secretion mediated by chloride channels, which relies on an intact basolateral Na^+/K^+ -ATPase function.^{43,44}

Methodology for the *ex vivo* opercular epithelia preparation followed our current methods.⁴⁵ Fish were anaesthetized with 2-phenoxyethanol (1:2000 v/v), sacrificed by decapitation and the cranium was cut longitudinally. The gills and other tissue remains were removed carefully and the epithelial skin covering the opercular bone were dissected out and transferred to fresh-gassed saline (99.7:0.3 O_2/CO_2) with the following composition (all values in mM): NaCl, 160; MgSO_4 , 0.93; NaH_2PO_4 , 3.0; CaCl_2 , 1.5; NaHCO_3 , 17.85; KCl, 3.0; glucose, 5.5; HEPES (pH 7.8), 5.0. The epithelia were overlaid onto a thin bore polythene net, protected between two parafilm gaskets and pinned over the circular aperture of a tissue holder (P2410, 0.20 cm^2 , Physiological Instruments, San Diego, USA), with the perimeter area lightly greased with vacuum silicone to minimize tissue edge damage. The mounted tissue was positioned between the two halves of the Ussing chamber (P2400, Physiological Instruments, San Diego, USA) with 4 mL of gassed saline at 22°C and gassed with a 99.7:0.3 O_2/CO_2 mix to provide oxygenation, good mixing by gas lift and pH control (pH = 7.8).

The preparations were left to stand for at least 60 min or until a steady basal measurement of bioelectrical variables was achieved. Measurement of the short circuit current (I_{sc} , $\mu\text{A cm}^{-2}$) was performed at symmetric conditions under voltage clamp



Scheme 1 Coupled enzymatic assay for Ca^{2+} -ATPase activity. PEP – phosphoenolpyruvate; P_i – inorganic phosphate.



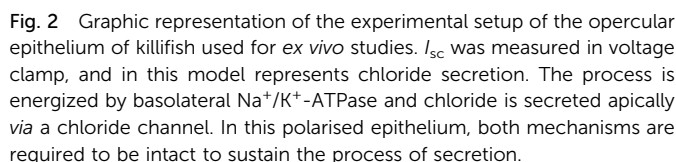
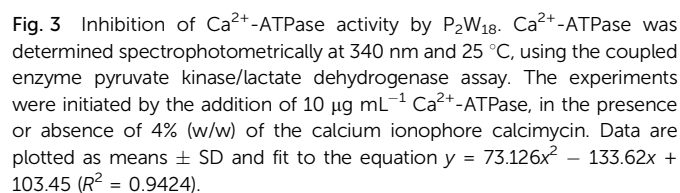


Fig. 2 Graphic representation of the experimental setup of the opercular epithelium of killifish used for *ex vivo* studies. I_{sc} was measured in voltage clamp, and in this model represents chloride secretion. The process is energized by basolateral Na^+/K^+ -ATPase and chloride is secreted apically *via* a chloride channel. In this polarised epithelium, both mechanisms are required to be intact to sustain the process of secretion.

Table 2 Inhibitory parameters of the POTs for SR Ca^{2+} -ATPase (IC_{50} values) activity and $\text{Na}^{+}/\text{K}^{+}$ -ATPase activity from basal membrane epithelia (effective time 50 ET_{50} and maximum inhibitory effects are calculated as the % of basal values). Inhibitory effect of different POTs applied basolaterally to the *ex vivo* preparation of the opercular epithelia of killifish mounted in Ussing chambers. Results are representative values for 3 independent experiments for each concentration (nd: not determined as no effect was observed after 30 minutes upon POT addition). Data showing the effect of ouabain for the $\text{Na}^{+}/\text{K}^{+}$ -ATPase inhibition is included as a positive control for the *ex vivo* system

POTs	Ca ²⁺ -ATPase	Na ⁺ /K ⁺ -ATPase	
Compound name	IC ₅₀ , (μM)	ET ₅₀ , (min (depending on concentration of compound))	Maximum inhibition, (%)
P ₂ W ₁₈	0.6	8.2 (0.5 μM)	86
		6.5 (1 μM)	99
		4.3 (10 μM)	100
TeW ₆	200	60 (10 μM)	10
CoW ₁₁ Ti	4	10 (10 μM)	75
SiW ₉	16	nd	nd
P ₂ W ₁₂	11	nd	nd
As ₂ W ₁₉	28	nd	nd
Se ₂ W ₂₉	0.3	6.5 (1 μM)	14
W ₂₂	68	nd	nd
AsW ₉	20	8.5 (10 μM)	66
Ouabain	—	3.2 (10 μM)	100

Similar moderate IC_{50} values for SR Ca^{2+} -ATPase activity were previously reported for two isostructural polyanions, decaniobate $[Nb_{10}O_{28}]^{6-}$ ($IC_{50} = 35 \mu M$) and decavanadate $[V_{10}O_{28}]^{6-}$ ($IC_{50} = 15 \mu M$).^{33,46} Both decaniobate and decavanadate showed a non-competitive inhibition for Ca^{2+} -ATPase activity



Inhibition of Ca²⁺-ATPase by POTs: *in vitro* study

The effect of nine different POTs (Fig. 1 and Table 1) on the activity of SR Ca^{2+} -ATPase from skeletal muscle was investigated for the first time. All of the investigated POTs inhibited Ca^{2+} -ATPase activity in a concentration dependent manner. The inhibitory power

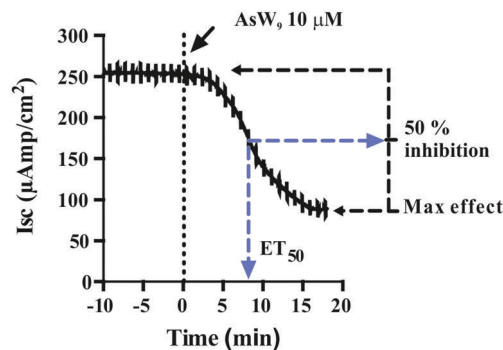


Fig. 5 The effect of the Keggin type AsW_9 applied in basolateral membranes at a concentration of $10 \mu\text{M}$ is shown. Original trace of the effect of short circuit current (I_{sc} , $\mu\text{A cm}^{-2}$) in the opercular epithelium of killifish mounted in Ussing chambers and kept under voltage clamp ($V_t = 0 \text{ mV}$). Effective time 50 (ET_{50}) and maximum inhibitory effects are calculated as the % of basal values. Both parameters were calculated for three individual independent experiments and used to generate Table 2. An arrow indicates the time of POT application and consequently the time point zero. Time with negative values represents stable basal control periods.

(providing information about inhibitor efficacy) and ET_{50} (providing information about inhibition velocity) are necessary to define the biological effects of POTs (Fig. 5 and Table 2). For the *ex vivo* studies, a positive control experiment was performed with the conventional Na^+/K^+ -ATPase inhibitor ouabain.^{43,49} Ouabain (at 10 μ M) showed a maximum inhibition value of 100% and an ET_{50} of 3.2 minutes (Fig. S1, ESI†). By inhibiting the basolateral Na^+/K^+ -ATPase activity, ouabain concomitantly prevents apical chloride secretion in the studied epithelia model as this process is energized by Na^+/K^+ -ATPase.^{43,49}

The addition of POTs to apical saline had no effect on I_{sc} and therefore ruling out chloride channels as putative POT targets, at least at POT concentrations up to 10 μM . The largest POT (in terms of volume and number of addenda atoms) under investigation, Se_2W_{29} , exhibited the highest inhibition ($\text{IC}_{50} = 0.3 \mu\text{M}$) of SR Ca^{2+} -ATPase activity during the *in vitro* study. However, used at the same concentration (1 μM), it was one of the weakest inhibitors (14% inhibition; Table 2 and Fig. 6) for the Na^+/K^+ -ATPase activity during the *ex vivo* study. In contrast, P_2W_{18} efficiently inhibited both the SR Ca^{2+} -ATPase *in vitro* ($\text{IC}_{50} = 0.6 \mu\text{M}$) and the Na^+/K^+ -ATPase *ex vivo* (99% inhibition) (Table 2 and Fig. 6). In fact, P_2W_{18} was demonstrated to be as potent as ouabain in inhibiting the Na^+/K^+ -ATPase activity (Table 2). The remaining studied POTs showed similar inhibitory effects *in vitro* and *ex vivo*. For example, the potential of TeW_6 to inhibit Ca^{2+} -ATPase (IC_{50} value of 200 μM) was as low as its effect against Na^+/K^+ -ATPase (inhibition of 10%; Table 2).

Both experiments (*in vitro* and *ex vivo*) clearly demonstrated the high selectivity of Se_2W_{29} for inhibiting the Ca^{2+} pump due to its rather sobering *ex vivo* results rendering this POT not the best choice to target the Na^+/K^+ -pump *in vivo*. The size (in terms of volume and number of addenda atoms) of this large POT could be one aspect affecting the kinetics of its cellular uptake, thus preventing the POT from targeting the enzyme. The mechanisms of POT uptake and their permeation through

Metallomics, 2018, 10, 287–295 | 291



Fig. 6 Inhibition (%) of the Na^+/K^+ -ATPase from basal membrane of the skin epithelia by two POTs P_2W_{18} and Se_2W_{29} . The inhibition rate of P_2W_{18} ($1 \mu\text{M}$) was 82% after 30 minutes (red), whereas for the most potent Ca^{2+} -ATPase inhibitor so far described, Se_2W_{29} ($\text{IC}_{50} = 0.3 \mu\text{M}$), a minor effect (green) was observed (14% inhibition, after 30 minutes). Perpendicular lines were used to calculate tissue resistance. As it can be observed, the *ex vivo* epithelia preparations retained integrity and selectivity after POT exposure.

epithelia still need to be clarified. The same selectivity pattern for inhibition of Ca^{2+} -ATPase activity ($\text{IC}_{50} = 400 \mu\text{M}$)³³ over Na^+/K^+ -ATPase ($\text{IC}_{50} = 1.5 \text{ mM}$)³⁴ was shown in previous studies for orthotungstate (HWO_4^-). Therefore, it seems that POT-mediated inhibition is pump-specific and there is no POT structure that is perfectly suited for all ion pumps in general. Moreover, the *ex vivo* results show that not only the affinity of the inhibitory compound is relevant, but also how the POT gains access to the inhibition site within an intracellular compartment, rendering the POT- Na^+/K^+ -ATPase interaction a complex one. The presented combination

of *in vitro* and *ex vivo* studies using two different models to study the effects of POTs on the activity of ATPases indicates the importance of establishing experimental conditions to be as close to the physiological environment as possible.

The majority of P-type ATPase inhibitors in therapy target the Na^+/K^+ -ATPase.^{32,48} These compounds, which are used for the treatment of several diseases such as heart failure, psychosis, malaria and bacterial infection, show inhibitory capacities resembling those of the here investigated POTs.⁴⁸ Only a few kinetic studies have been described so far testing POTs as P-type ATPase inhibitors.^{24,32,42,46} The *in vitro* inhibition of Na^+/K^+ -ATPase by the Keggin POTs $\text{H}_3\text{PW}_{12}\text{O}_{40}$ and $\text{H}_4\text{SiW}_{12}\text{O}_{40}$ was previously described reporting IC_{50} values between 3 to $4 \mu\text{M}$ ³² although information about the type of inhibition and the mechanism of action are still lacking. In this study the comparable IC_{50} value for the isostructural Keggin POT CoW_{11}Ti ($\text{IC}_{50} = 4 \mu\text{M}$) was observed.

Protein interactions and structure/function features of POTs

In order to decipher specific features of the nine POTs that are responsible for the inhibition of Ca^{2+} -ATPase, we correlated the POT parameters like size and charge density with their IC_{50} values of inhibition (Fig. 7A and B). No correlation was found when considering all nine POTs and thus all determined IC_{50} values. However, when taking only into account the high affinity POTs, exhibiting IC_{50} values lower than $16 \mu\text{M}$, we observed a correlation between their activity (IC_{50} value) and their charge density, which was defined as charge of the POT divided by its number of W atoms (Fig. 7A) as well as by the volume of POT anion (Fig. 7B). As can be deduced from this data, POTs such as Se_2W_{29} and P_2W_{18} with a low charge density (Fig. 7A and B) favored the inhibition of Ca^{2+} -ATPase activity indicating that besides electrostatic interactions also steric interactions (depending on the shape complementarity between the POT and the inhibition site) might play important roles in the successful inhibition of Ca^{2+} -ATPase.

For the *ex vivo* results (Na^+/K^+ -ATPase) no correlation between the ET_{50} values and POT charge density was observed.

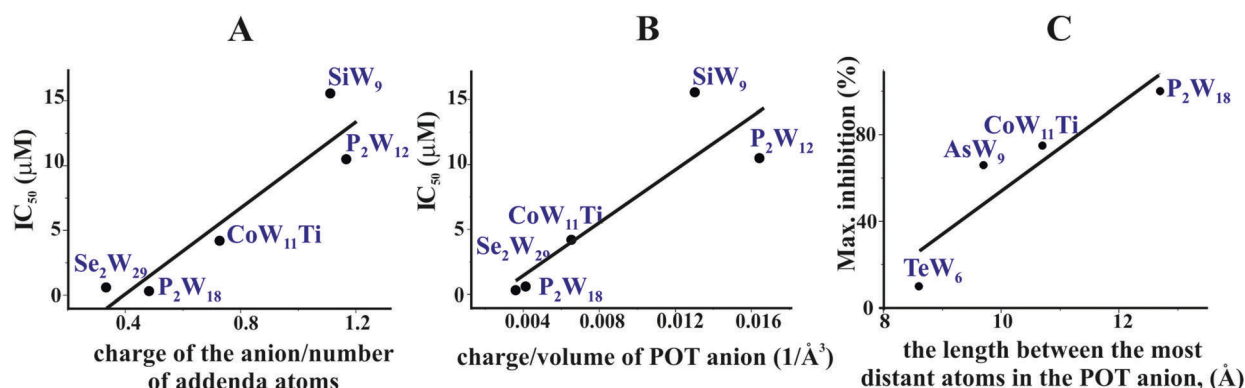


Fig. 7 Structure–activity correlations of different POTs for ATPases inhibition. (A) Correlation between the IC_{50} values of five POTs (IC_{50} lower than $16 \mu\text{M}$) of Ca^{2+} -ATPase inhibition and their charge density expressed as charge of the POT divided by its number of W atoms. (B) Correlation between the IC_{50} values of five POTs (IC_{50} lower than $16 \mu\text{M}$) against Ca^{2+} -ATPase and the charge density expressed as charge of the POT divided by its volume (in \AA^{-3}). (C) Correlation between the percentage of maximum inhibition of four POTs (applied with the same concentration of $10 \mu\text{M}$) against Na^+/K^+ -ATPase and POT size expressed as the length between the most distant atoms in the POT anion (in \AA).

- Science. NATO Science Series (Series II: Mathematics, Physics and Chemistry)*, ed. J. J. Borrás-Almenar, E. Coronado, A. Müller, M. Pope, Springer, Dordrecht, 2003, vol. 98, pp. 381–416.
- 5 M. A. Moussawi, N. Leclerc-Laronze, S. Floquet, P. A. Abramov, M. N. Sokolov, S. Cordier, A. Ponchel, E. Monflier, H. Bricout, D. Landy, M. Haouas, J. Marrot and E. Cadot, Polyoxometalate, cationic cluster, and γ -cyclodextrin: from primary interactions to supramolecular hybrid materials, *J. Am. Chem. Soc.*, 2017, **139**, 12793–12803.
 - 6 A. Proust, R. Thouvenot and P. Gouzerh, Functionalization of polyoxometalates: towards advanced applications in catalysis and materials science, *Chem. Commun.*, 2008, 1837–1852.
 - 7 A. Bijelic and A. Rompel, The use of polyoxometalates in protein crystallography—An attempt to widen a well-known bottleneck, *Coord. Chem. Rev.*, 2015, **299**, 22–38.
 - 8 A. Bijelic and A. Rompel, Ten Good reasons for the use of the tellurium-centered Anderson–Evans polyoxotungstate in protein crystallography, *Acc. Chem. Res.*, 2017, **50**, 1441–1448.
 - 9 C. Molitor, A. Bijelic and A. Rompel, The potential of hexatungstotellurate(vi) to induce a significant entropic gain during protein crystallization, *IUCr*, 2017, **4**, 734–740.
 - 10 A. Bijelic, C. Molitor, S. G. Mauracher, R. Al-Oweini, U. Kortz and A. Rompel, Hen egg-white lysozyme crystallisation: protein stacking and structure stability enhanced by a tellurium(vi)-centred polyoxotungstate, *ChemBioChem*, 2015, **16**, 233–241.
 - 11 S. G. Mauracher, C. Molitor, R. Al-Oweini, U. Kortz and A. Rompel, Crystallization and preliminary X-ray crystallographic analysis of latent isoform PPO4 mushroom (*Agaricus bisporus*) tyrosinase, *Acta Crystallogr.*, 2014, **F70**, 263–266.
 - 12 S. G. Mauracher, C. Molitor, R. Al-Oweini, U. Kortz and A. Rompel, Latent and active *ab*PPO4 mushroom tyrosinases cocrystallized with hexatungstotellurate(vi) in a single crystal, *Acta Crystallogr.*, 2014, **D70**, 2301–2315.
 - 13 C. Molitor, S. G. Mauracher and A. Rompel, Crystallization and preliminary crystal structure analysis of latent, active and recombinantly expressed aurone synthase – a polyphenol oxidase – from *Coreopsis grandiflora*, *Acta Crystallogr.*, 2015, **F71**, 746–751.
 - 14 C. Molitor, S. G. Mauracher and A. Rompel, Aurone synthase is a catechol oxidase with hydroxylase activity and provides insights into the mechanism of plant polyphenol oxidases, *Proc. Natl. Acad. Sci. U. S. A.*, 2016, **113**, E1806–E1815.
 - 15 C. Molitor, A. Bijelic and A. Rompel, *In situ* formation of the first proteinogenically functionalized $[\text{TeW}_6\text{O}_{24}\text{O}_2(\text{Glu})]^{7-}$ structure reveals unprecedented chemical and geometrical features of the Anderson-type cluster, *Chem. Commun.*, 2016, **52**, 12286–12289.
 - 16 B. Hasenknopf, Polyoxometalates: introduction to a class of inorganic compounds and their biomedical applications, *Front. Biosci.*, 2005, **10**, 275–287.
 - 17 T. Yamase, Polyoxometalates active against tumors, viruses, and bacteria, in *Biomedical Inorganic Polymers*, ed. W. E. G. Müller, X. Wang, H. C. Schröder, Springer, Berlin, Heidelberg, Mainz, 2013, pp. 65–116.
 - 18 H. Stephan, M. Kubeil, F. Emmerling and C. E. Müller, Polyoxometalates as versatile enzyme inhibitors, *Eur. J. Inorg. Chem.*, 2013, 1585–1594.
 - 19 S. Y. Lee, A. Fiene, W. Li, T. Hanck, K. A. Brylev, V. E. Fedorov, J. Lecka, A. Haider, H. J. Pietzsch, H. Zimmermann, J. Sévigny, U. Kortz, H. Stephan and C. E. Müller, Polyoxometalates—potent and selective ecto-nucleotidase inhibitors, *Biochem. Pharmacol.*, 2015, **93**, 171–181.
 - 20 H. U. V. Gerth, A. Rompel, B. Krebs, J. Boos and C. Lanvers-Kaminsky, Cytotoxic effects of novel polyoxotungstates and a platinum compound on human cancer cell lines, *Anti-Cancer Drugs*, 2005, **16**, 101–106.
 - 21 A. Galani, V. Tsitsias, D. Stellas, V. Psycharis, C. P. Raptopoulou and A. Karaliota, Two novel compounds of vanadium and molybdenum with carnitine exhibiting potential pharmacological use, *J. Inorg. Biochem.*, 2015, **142**, 109–117.
 - 22 S. Treviño, D. Velázquez-Vázquez, E. Sánchez-Lara, A. Diaz-Fonseca, J. A. Flores-Hernandez, A. Pérez-Benítez, E. Brambila-Colombres and E. González-Vergara, Metforminium decavanadate as a potential metallopharmaceutical drug for the treatment of diabetes mellitus, *Oxid. Med. Cell. Longevity*, 2016, 6058705.
 - 23 T. L. Turner, V. H. Nguyen, C. C. McLauchlan, Z. Dymon, B. M. Dorsey, J. D. Hooker and M. A. Jones, Inhibitory effects of decavanadate on several enzymes and *Leishmania tarentolae* *in vitro*, *J. Inorg. Biochem.*, 2012, **108**, 96–104.
 - 24 M. Aureliano, Decavanadate toxicology and pharmacological activities: V_{10} or V_1 , Both or None?, *Oxid. Med. Cell. Longevity*, 2016, 6103457.
 - 25 F. Zhai, X. Wang, D. Li, H. Zhang, R. Li and L. Song, Synthesis and biological evaluation of decavanadate $\text{Na}_4\text{Co}(\text{H}_2\text{O})_6\text{V}_{10}\text{O}_{28} \cdot 18\text{H}_2\text{O}$, *Biomed. Pharmacother.*, 2009, **63**, 51–55.
 - 26 R. Raza, A. Matin, S. Sarwar, M. Barsukova-Stuckart, M. Ibrahim, U. Kortz and J. Iqbal, Polyoxometalates as potent and selective inhibitors of alkaline phosphatases with profound anticancer and amoebicidal activities, *Dalton Trans.*, 2012, **41**, 14329–14336.
 - 27 L. De Matteis, S. G. Mitchell and J. M. de la Fuente, Supramolecular antimicrobial capsules assembled from polyoxometalates and chitosan, *J. Mater. Chem. B*, 2014, **2**, 7114–7117.
 - 28 A. Bijelic, M. Aureliano and A. Rompel, The antibacterial activity of polyoxometalates: structures, antibiotic effects and future perspectives, *Chem. Commun.*, DOI: 10.1039/c7cc07549a.
 - 29 A. Blazevic and A. Rompel, The Anderson–Evans polyoxometalate: From inorganic building blocks via hybrid organic–inorganic structures to tomorrows “Bio-POM”, *Coord. Chem. Rev.*, 2016, **307**, 42–64.
 - 30 L. de Meis and A. L. Vianna, Energy interconversion by the Ca^{2+} -dependent ATPase of the sarcoplasmic reticulum, *Annu. Rev. Biochem.*, 1979, **48**, 275–292.
 - 31 C. Toyoshima, M. Nakasako, H. Nomura and H. Ogawa, The structural basis for coupling of Ca^{2+} transport to ATP hydrolysis by the sarcoplasmic reticulum Ca^{2+} -ATPase, *Nature*, 2004, **405**, 647–655.
 - 32 L. Yatime, M. J. Buch-Pedersen, M. Musgaard, J. P. Morth, A.-M. L. Winther, B. P. Pedersen, C. Olesen, J. P. Andersen,



- B. Vilsen, B. Schiøtt, M. G. Palmgren, J. V. Møller, P. Nissen and N. Fedosova, P-type ATPases as drug targets: tools for medicine and science, *Biochim. Biophys. Acta*, 2009, **1787**, 207–220.
- 33 G. Fraqueza, C. A. Ohlin, W. H. Casey and M. Aureliano, Sarcoplasmic reticulum calcium ATPase interactions with decanionate, decavanadate, vanadate, tungstate and molybdate, *J. Inorg. Biochem.*, 2012, **107**, 82–89.
- 34 M. B. Colović, D. V. Bajuk-Bogdanovic, N. S. Avramovic, I. D. Holclajtner-Antunovic, N. S. Bošnjaković-Pavlovic, V. M. Vasić and D. Z. Krstić, Inhibition of rat synaptic membrane Na^+/K^+ -ATPase and ecto-nucleoside triphosphate diphosphohydrolases by 12-tungstosilicic and 12-tungstophosphoric acid, *Bioorg. Med. Chem.*, 2011, **19**, 7063–7069.
- 35 *Inorganic Chemistry*, ed. A. P. Ginsberg, Wiley, New-York, 1990, vol. 27, pp. 71–132.
- 36 K. J. Schmidt, G. J. Schrobilgen and J. F. Sawyer, Hexasodium hexatungstotellurate(vi) 22-hydrate, *Acta Crystallogr.*, 1986, **C42**, 1115–1118.
- 37 W. Kraus, H. Stephan, A. Röllich, Z. Matějka and G. Reck, $\text{K}_6\text{H}_2[\text{TiW}_{11}\text{CoO}_{40}]\cdot 13\text{H}_2\text{O}$, with a monotitanoundecatungstocobaltate(II) anion, *Acta Crystallogr.*, 2005, **E61**, i35–i37.
- 38 C. Tourné, A. Revel, G. Tourné and M. Vendrell, Heteropolytungstates containing elements of phosphorus family with degree of oxidation(III) or (V)—identification of species having composition X_2W_{19} and XW_9 ($\text{X} = \text{P}, \text{As}, \text{Sb}, \text{Bi}$) and relation to those with composition XW_{11} , *C. R. Seances Acad. Sci., Ser. C*, 1973, **277**, 643–645.
- 39 U. Kortz, M. G. Savelieff, B. S. Bassil and M. H. Dickman, A large, novel polyoxotungstate: $[\text{As}_6^{\text{III}}\text{W}_{65}\text{O}_{217}(\text{H}_2\text{O})_7]^{26-}$, *Angew. Chem., Int. Ed.*, 2001, **40**, 3384–3386.
- 40 J. Gao, J. Yan, S. Beeg, D.-L. Long and L. Cronin, One-pot versus sequential reactions in the self-assembly of gigantic nanoscale polyoxotungstates, *J. Am. Chem. Soc.*, 2013, **135**, 1796–1805.
- 41 H. N. Miras, J. Yan, D.-L. Long and L. Cronin, Structural evolution of “S”-shaped $[\text{H}_4\text{W}_{22}\text{O}_{74}]^{12-}$ and “§”-shaped $[\text{H}_{10}\text{W}_{34}\text{O}_{116}]^{18-}$ isopolyoxotungstate clusters, *Angew. Chem., Int. Ed.*, 2008, **47**, 8420–8423.
- 42 M. Aureliano, F. Henao, T. Tiago, R. O. Duarte, J. J. G. Moura, B. Baruah and D. C. Crans, Sarcoplasmic reticulum calcium ATPase is inhibited by organic vanadium coordination compounds: pyridine-2,6-dicarboxylatodioxovanadium(V), BMOV, and an amavadin analogue, *Inorg. Chem.*, 2008, **47**, 5677–5684.
- 43 K. J. Karnaky Jr, K. J. Degnan and J. A. Zadunaisky, Chloride transport across isolated opercular epithelium of killifish: a membrane rich in chloride cells, *Science*, 1977, **195**, 203–205.
- 44 J. A. Zadunaisky, The chloride cell: the active transport of chloride and the paracellular pathways, *Fish Physiology*, XB, ed. W. S. Hoar, D. J. Randall, Academic Press, New York, 1984, 129–176.
- 45 J. A. Martos-Sitcha, G. Martínez-Rodríguez, J. M. Mancera and J. Fuentes, AVT and IT regulate ion transport across the opercular epithelium of killifish (*Fundulus heteroclitus*) and gilthead sea bream (*Sparus aurata*), *Comp. Biochem. Physiol., Part A: Mol. Integr. Physiol.*, 2015, **182**, 93–101.
- 46 G. Fraqueza, L. A. E. Batista de Carvalho, M. Paula, M. Marques, L. Maia, C. André Ohlin, W. H. Casey and M. Aureliano, Decavanadate, decanionate, tungstate and molybdate interactions with sarcoplasmic reticulum Ca^{2+} -ATPase: quercetin prevents cysteine oxidation by vanadate but does not reverse ATPase inhibition, *Dalton Trans.*, 2012, **41**, 12749–12758.
- 47 S. Hua, G. Inesi and C. Toyoshima, Distinct topologies of mono- and decavanadate binding and photo-oxidative cleavage in the sarcoplasmic reticulum ATPase, *J. Biol. Chem.*, 2000, **275**, 30546–30550.
- 48 M. Aureliano, G. Fraqueza and C. A. Ohlin, Ion pumps as biological targets for decavanadate, *Dalton Trans.*, 2013, **42**, 11770–11777.
- 49 K. J. Degnan, K. J. Karnaky, Jr. and J. A. Zadunaisky, Active chloride transport in the in vitro opercular skin of a teleost (*Fundulus heteroclitus*), a gill-like epithelium rich in chloride cells, *J. Physiol.*, 1977, **271**, 155–191.